Biosensors and Bioelectronics 26 (2010) 477–484

Contents lists available at ScienceDirect

Biosensors and Bioelectronics

journal homepage: www.elsevier.com/locate/bios

Enzyme-based choline and L-glutamate biosensor electrodes on silicon microprobe arrays

O. Frey[a,*], T. Holtzman[b], R.M. McNamara[b], D.E.H. Theobald[b], P.D. van der Wal[a], N.F. de Rooij[a], J.W. Dalley[b], M. Koudelka-Hep[a]

[a] Ecole Polytechnique Fédérale de Lausanne (EPFL), Institute of Microengineering (IMT), Sensors, Actuators and Microsystems Laboratory (SAMLAB), Rue Jaquet-Droz 1, 2000 Neuchâtel, Switzerland

[b] University of Cambridge, Department of Experimental Psychology, Downing Site, Cambridge, UK

ARTICLE INFO

Article history:
Received 16 April 2010
Received in revised form 9 July 2010
Accepted 19 July 2010
Available online 11 August 2010

Keywords:
Biosensor
Choline
Glutamate
Microprobe array
Enzyme immobilisation

ABSTRACT

Brain-implantable microprobe arrays, 6.5 mm shaft-length, incorporating several recessed Pt microelectrodes (50 μm × 150 μm) and an integrated Ag/AgCl reference electrode fabricated by silicon micromachining dry etching techniques (DRIE) are described. The microelectrodes are coated by an enzyme membrane and a semi-permeable *m*-phenylenediamine layer for the selective detection of the neurotransmitters choline and L-glutamate at physiologically relevant concentrations. The functionalisation is based on electrochemically aided adsorption (EAA) combined with chemical co-cross-linking using glutaraldehyde and electrochemical polymerisation, respectively. These deposition methods are fully compatible with the fabricated microprobe arrays for the simultaneous detection of several analytes in different brain target areas. They are spatially controlled and allow fabricating biosensors on several microelectrodes in parallel or providing a cross-talk-free coating of closely spaced microelectrodes with different enzyme membranes. A sensitivity of $132 \pm 20\ \mu A\ mM^{-1}\ cm^{-2}$ for choline and $95 \pm 20\ \mu A\ mM^{-1}\ cm^{-2}$ for L-glutamate with limits of detections below 0.5 μM was obtained. The results of *in vitro* and *in vivo* experiments confirm the functional viability of the choline and L-glutamate biosensors.

1. Introduction

There is undisputed need for the measurement of neurochemical substances in brain tissue. Its field of application is widely spread and ranges from basic research on the functional and anatomical mapping of the brain, over the inter-neuronal monitoring of larger circuitry to experimental psychology trying to establish a link between observable behaviour and concentration variations of specific molecules in dedicated brain regions. The major, long-term goal is certainly the understanding and successful development of remedies for several neurological disorders such as schizophrenia, epilepsy or Parkinson's disease. The neurotransmitters choline (a surrogate marker of released acetylcholine) and L-glutamate (the primary excitatory neurotransmitter in the brain) play a major role in all these fields.

Observing recent developments, sensing probes trend to smaller dimensions and an increased number of electrodes per probe permitting analysis within smaller brain structures at reduced brain damage and a simultaneous recording of one or multiple analytes at different locations. This offers a much more three-dimensional, network-oriented interpretation of local brain circuitry.

Most adequate regarding these aspects are microprobes fabricated by standard microtechnology processes equipped with multiple enzyme-based electrochemical biosensors. Even if microdialysis probes posses an unequivocal limit of detection, sensitivity and chemical selectivity when coupled with high-performance detection techniques (Guerrieri and Palmisano, 2001; Lada et al., 1997), they have limitations in spatial and temporal resolution (Fillenz, 2005) and tissue damage upon insertion is likely (Khan and Michael, 2003). Microwires are very small and suitable to reach deep brain structures, but have restrictions to record from different locations. Assembled bundles creating tetrodes (Gray et al., 1995) or arrays (Ulbert et al., 2001; Musallam et al., 2007) mostly suffer from a limited accuracy and reproducibility of the relative electrode positioning and the capacity of only one tip-electrode per wire.

Microfabricated probes were presented by several groups using insulated substrates as ceramics (Burmeister et al., 2000, 2002) or passivated silicon. For the latter, different approaches are applied

* Corresponding author. Tel.: +41 327205654; fax: +41 327205711.
E-mail addresses: olivier.frey@epfl.ch (O. Frey), th247@cam.ac.uk (T. Holtzman), rmm59@cam.ac.uk (R.M. McNamara), dt237@cam.ac.uk (D.E.H. Theobald), peter.vanderwal@epfl.ch (P.D. van der Wal), nico.derooij@epfl.ch (N.F. de Rooij), jwd20@cam.ac.uk (J.W. Dalley), mkoudelka@eblcom.ch (M. Koudelka-Hep).

0956-5663/$ – see front matter © 2010 Elsevier B.V. All rights reserved.
doi:10.1016/j.bios.2010.07.073

to structure the microprobes. These include boron-doping used as wet etch-stop (Wise et al., 1970; Najafi et al., 1985; Takahashi and Matsuo, 1984; Leong et al., 1990), combined dry and wet etching of silicon (Kewley et al., 1997; Yoon et al., 2000), or only dry etching procedures (Errachid et al., 2001; Wassum et al., 2008; Herwik et al., 2009) including also the use of SOI substrates (Ensell et al., 2000; Norlin et al., 2002; Cheung et al., 2003). Each probe is patterned with multiple thin-film electrodes along the length of the shaft adapted to specific experimental requirements and allows parallel recordings from several sites on a single, implanted microprobe. Arranging different probes to combs and arrays enables two- or even three-dimensional mapping of larger areas in the brain. Recently, such kind of microprobes became also commercially available (NeuroNexus Tech., USA).

The biosensors used on these microprobes are mostly based on the amperometric detection of peroxide produced by the enzyme catalysed reaction of the specific neurotransmitter and oxygen (Wilson and Gifford, 2005; Qin et al., 2008; Robinson et al., 2008). The involved enzyme choline oxidase (ChoOx) for the detection of choline or L-glutamate oxidase (GluOx) for L-glutamate is immobilised on the electrode site in a post-processing step (Sarma et al., 2009; Hanefeld et al., 2009). Deposition techniques for the fabrication of reliable multi-analyte biosensors on microelectrode arrays require an excellent spatial control and reproducibility.

A variety of deposition methods exist, mostly developed in parallel with the electrode fabrication. Dip-coating for example is primarily used for microwires. Multiple immersions in a solution adsorb the enzyme on the electrode surface, where it is immobilised either using a cross-linking agent, such as glutaraldehyde (GA) (Hu et al., 1994; Xin and Wightman, 1997; Schuvailo et al., 2005) or PEGDGE (Garguilo et al., 1993; Kulagina et al., 1999; Mikeladze et al., 2002; Mitala and Michael, 2006), or in a polymer (Ryan et al., 1997). For multi-electrode probes and the deposition of discrete layers deposited close to (but kept distinct from) neighbouring layers, this approach may not be suitable.

Dispensing small volumes directly onto the electrode site (Burmeister et al., 2002; Niwa et al., 1998) allows better spatial control but to ensure reproducibility and a controlled deposition, high-priced low-volume dispensing equipment is required (Newman et al., 1992).

Considering electrochemically based deposition methods, spatial control is inherent and serial deposition on several electrodes (drop-coating) is replaced by a parallel coating only formed at the appropriately biased electrodes. A variety of polymers used for enzyme immobilisation were presented in the last years (for review see Cosnier, 2003). One example is poly(pyrrole) (PPy, Yoshida et al., 1995; Cosnier et al., 1997), a rather dense matrix increasing the response time of the sensor by up to 1 min. Alternatively, poly(phenylenediamine) (PPD) is used for the fabrication of implantable biosensors (Malitesta et al., 1990; Lowry et al., 1998; O'Neill et al., 2008). Film-thickness estimations for PPD layers are in the region of 10–30 nm and therefore limiting in the amount of enzyme loadable. Nevertheless, these two polymers also show interference-rejection properties against endogenous, electroactive molecules such as ascorbic acid or dopamine present in the extracellular fluid. Especially the semi-permeable PPD layer possesses excellent interference-rejection characteristics and additionally, protects the electrode surface from fouling (Geise et al., 1991).

Electrochemically aided adsorption (EAA; Johnson, 1991; Lee et al., 1991; Strike et al., 1995; Matsumoto et al., 2002) or a similar approach using electrodeposition paints (Kurzawa et al., 2002) are further methods for enzyme immobilisation. They were used in the past for different enzymes on planar single microelectrodes. EAA allows combining an electrochemical technique with the good sensor characteristics observed using chemical co-cross-linking with glutaraldehyde. It is spatially controlled and allows highly parallel deposition on multiple sites or the incorporation of different enzymes at different locations on the same microprobe. Therefore the method is very suitable for three-dimensional microelectrode arrays. In addition, the majority of the established anti-interference schemes are applicable before or after immobilisation.

In this paper, we present the fabrication of silicon microprobe arrays with multiple, recessed Pt thin-film microelectrodes and an integrated Ag/AgCl reference electrode on each shaft. The biosensor functionalisation is optimised for choline and L-glutamate biosensors using an EAA protocol offering a completely array-compatible method including reliable enzyme immobilisation as well as anti-interference layer deposition. Results of an extended *in vitro* assessment and functional *in vivo* tests confirm adequate characteristics for further *in vivo* use.

2. Materials and methods

2.1. Layout of the silicon microprobes

The latest developments in silicon microtechnology – especially in the field of plasma enhanced anisotropic dry etching techniques (DRIE) – offer increased possibility and flexibility in design of experiment-tailored microprobe array configurations regarding dimensions and arrangements of electrodes and shafts and their accurate implementation.

In this contribution, the microprobes are designed for recordings in the medial prefrontal cortex (mPFC) of the rat brain. Therefore the dimensions of the microprobe were chosen to be 6.5 mm in length, 100 μm in width with an allover thickness of 30–100 μm. Two 50 μm × 150 μm thin-film Pt microelectrodes are integrated in a 10-μm lowered cavity (recess), separated by 200 μm and located at 500 μm from the tip (see supplementary data, Fig. SD1). The recess anchors and protects the enzymatic membrane on the electrodes during tissue insertion and removal. Additionally, a third, non-recessed electrode with dimensions of 40 μm × 500 μm is positioned further backwards. Additional electrodes can be integrated on the same microprobe at application-desired positions with minor widening of the shaft.

2.2. Fabrication of the silicon microprobes

The microprobes are fabricated starting with a 300 μm (1 0 0) silicon wafer. A first mask is transferred to a previously grown thermal oxide (200 nm) and a recess of 10 μm is etched using KOH (Fig. 1a). The interconnection lines are laid across the inclined side walls that appear during the KOH etch (Madou, 1997). An adapted design leads to the shape of the cavity illustrated in Fig. SD1

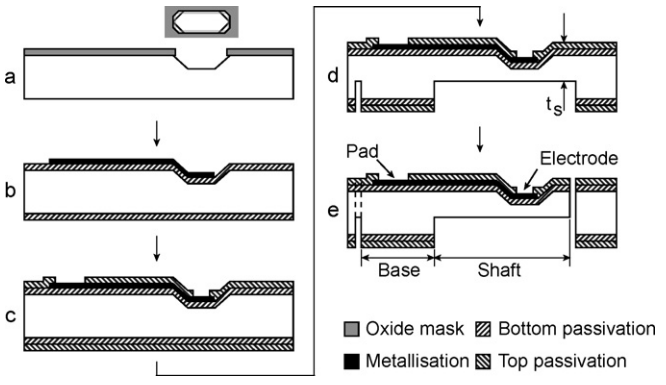

Fig. 1. Complete fabrication procedure for silicon microprobe arrays (see text for details).

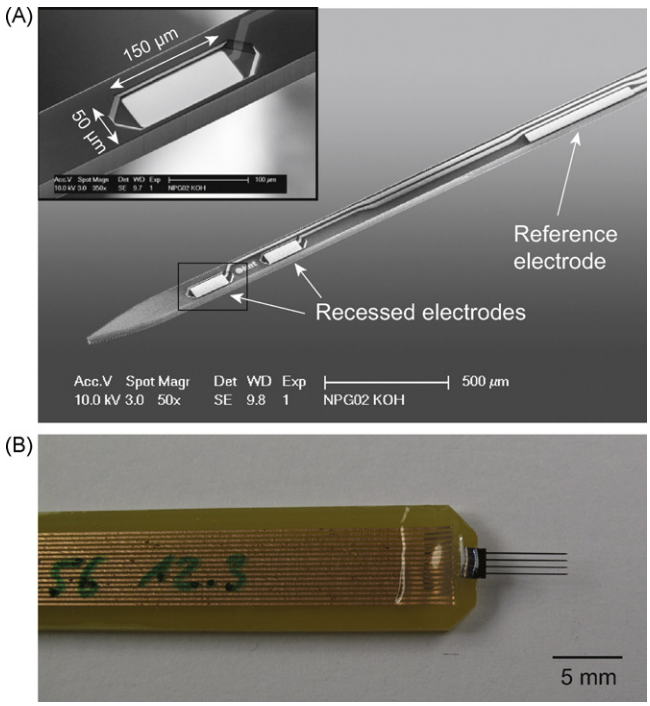

Fig. 2. SEM micrograph of the front part of the shaft of the fabricated silicon microprobe and close up view of the KOH-recessed Pt microelectrode. The metal interconnection track is laid across the inclined side wall appearing after the KOH etch.

(enlarged tip) and Fig. 2-A in Section 3 that essentially decreases the amount of space required in the lateral dimension (=lower-width probes).

Subsequently, 200 nm of thermally grown dry oxide and 200 nm LPCVD silicon nitride layers are successively deposited as bottom passivation. The metallisation (20 nm of Ta and 130 nm of Pt) is patterned by a lift-off process using a combination of thick photoresist AZ4562 (AZ Electronic Materials GmbH, Germany) and LOR 3B (MicroChem Corp., Newton, USA). A total resist thickness of about 8 μm is required to reliably cover the edges of the recesses and produce well-defined metal structures (b). A second 200 nm LPCVD silicon nitride layer and 200 nm PECVD oxide layer are used as top passivation that is opened at the recording sites and bonding pads by reactive ion etching (RIE) and a H_3PO_4 dip (10 min at 160 °C; Fig. 1c). The microprobes are formed by a first thinning from the backside by DRIE towards the intended shaft thickness t_S and a second DRIE etch from the front side to shape the needle contour. For both etching steps, thick photoresist is used as mask (d and e). Small joints are retaining the microprobes in the remaining wafer grid, where they are stored and released before packaging.

Different types of probes were realised: single probes and 4-shaft combs grouping single probes at a pitch of 550 μm and 2 mm (see Fig. SD1). Additionally, combs for 3D-array integration were fabricated (for details see Aarts et al., 2008; Herwik et al., 2009). For acute measurements in anaesthetised rats, the probes are attached to custom-made, stick-like printed circuit boards (PCB, 5–8 mm × 60 mm). Bonding pads, bonding wires and metal lines on the PCB are embedded in epoxy glue to mechanically protect and electrically insulate the connections. The assembly is simple, convenient and compatible with conventional stereotaxic frames.

The larger electrode (40 μm × 500 μm) located 2 mm from the tip is transformed to an Ag/AgCl reference electrode. First a silver layer of 4–5 μm is galvanostatically grown on the Pt surface using a commercial deposition bath (Silver Glo, Rohm and Haas, Buchs, Switzerland). About 1 μm of the surface is electrochemically transformed into AgCl using again a galvanostatic procedure in a 50 mM KCl solution.

2.3. Chemicals

The following chemicals were purchased from Sigma–Aldrich (Fluka Chemika), Buchs, Switzerland: choline oxidase from *Alcaligenes* sp., bovine serum albumin (BSA), 3-aminopropyltriethoxysilane (APTES, 99%), Triton X-100, glutaraldehyde solution (25%, w/v in water) and *m*-phenylenediamine.

Following calibration stock solutions were prepared (dissolved in DI-water): choline (10 mM; from choline chloride, Fluka), L-glutamate (10 mM; from L-glutamic acid monosodium salt monohydrate, Fluka), dopamine (2 mM; from dopamine hydrochloride, Sigma) and ascorbic acid (200 mM; Fluka).

Home-made 0.01 M phosphate buffered saline (PBS) solution consisted of (for 1 l PBS): 9 g NaCl (Fluka), 1.367 g $Na_2HPO_4{\cdot}2H_2O$ (Merck) and 0.368 g $NaH_2PO_4{\cdot}H_2O$ (Merck), adjusted to pH 7.2.

L-Glutamate oxidase from *Streptomyces* sp. was purchased from Yamasa Corp., Japan, H_2SO_4 from Merck.

2.4. Functionalisation

Step 1: The surface of the platinum electrodes was first cleaned and electrochemically assessed by cyclic voltammetry in deaerated 1 M H_2SO_4. The electrodes were scanned 15 times over a range of −0.2 to 1.35 V vs. an Ag/AgCl reference electrode (Metrohm Schweiz AG, Zofingen, Switzerland) with 100 mV/s.

Step 2: Prior to the enzyme immobilisation, the microprobes were pretreated by a vapour silanisation procedure in a petri dish together with 4–5 drops (∼50 μl) of APTES and left there for 2 h.

Step 3: The immobilisation of the appropriate enzyme was performed out of a 1 ml-volume: 15 mg of BSA and the enzyme were dissolved in 940 μl PBS. 4.5 mg were used for choline oxidase (∼45 units), ∼3 mg for L-glutamate oxidase (50 units), respectively. Additionally, 20 μl of Triton X-100 solution (3 g/l) was added to the mixture to increase the wettability, when the microprobe is immersed into the solution. Without the surfactant, occasionally, air bubbles were entrapped in the electrode recess. Once thoroughly dissolved using a magnetic stirrer, 40 μl of glutaraldehyde (GA) was added just before the deposition giving a concentration of 1% (v/v).

For the deposition, a platinum wire and an Ag/AgCl wire were used as counter and reference electrode, respectively. Directly after microprobe immersion, the deposition protocol is started by applying 25 pulses, each pulse consisting of 5 s at 1.8 V followed by 10 s at 0.4 V.

After deposition, the electrodes were rinsed with DI-water and left to air-dry for 1–2 h. Multiple electrodes on a comb are coated in parallel. Two different enzymes are immobilised consecutively in two different solutions by applying the above-described procedure (step 3) for each electrode.

2.5. Anti-interference scheme

Selectivity of the biosensor was achieved by a two-way approach: the application of a semi-permeable layer blocking interferants by size discrimination and using the differential method:

Step 4: An *m*-polyphenylenediamine layer was deposited by electropolymerisation from a monomer solution of 100 mM *m*-PD by cyclic voltammetry. The optimised protocol consisted of 15 cycles from 0 to 0.9 V vs. Ag/AgCl with a scan rate of 50 mV/s performed after the immobilisation of the enzyme layer.

Step 5: To implement the differential method, the second electrode on the same microprobe placed at a distance of 200 μm from

the first active one was coated with a membrane containing only the BSA protein (19 mg/ml in the deposition solution). The deposition was performed after the enzyme immobilisation on the first electrode and followed the same protocol. The inactive protein membrane is required to generate an equal diffusion barrier for the molecules to the electrode surface and match the temporal recording behaviour of the two microelectrodes. Therefore the *m*-PPD layer was also applied on the inactive electrode and deposited in parallel to the active one. After polymerisation the electrodes were kept for 15 h in PBS solution at room temperature.

2.6. In vitro calibration set-up

Calibration measurements were performed in PBS or artificial extracellular fluid (aECF) at a temperature of 37 °C using an Ag/AgCl reference electrode and a platinum wire (both from Metrohm) as the counter electrode. The biosensor was connected to an electrochemical recording system (PalmSens expanded by a 8-channel multiplexer, Palm Instruments BV Netherlands or eDAQ QuadStat, Australia) using a three-electrode configuration. A potential of 0.7 V vs. Ag/AgCl was applied. The calibration was started as soon as a constant background current was achieved (20–30 min). Then, aliquots of neurotransmitter were consecutively added in 2×10 μM steps followed by manual stirring. Biosensors were also tested against ascorbic acid (AA) and dopamine (DA). Between measurements the biosensors were stored in PBS at 4 °C.

2.7. In vivo measurement set-up

Male Lister hooded rats (200–400 g) were anaesthetised with urethane (1.5 g/kg; intraperitoneal) and placed in a flat-skull position in a stereotaxic frame (incisor bar −3.3 mm relative to the interaural plane). All animal experiments were carried out in accordance with the European Communities Council Directive 86/609/EEC. The soft tissues overlying the skull were removed and a craniotomy was performed to expose regions of the frontal cortex. The dura mater was removed prior to insertion of the microprobe so as to minimise mechanical deformation of the brain tissue during microprobe insertions. Relative to the skull landmark bregma, probes were inserted vertically targeted to the medical prefrontal cortex (AP +2.5–3.5, ML 1.5, DV 5.5).

For local drug delivery, the biosensor microprobes were assembled in two ways: (a) with 31-gauge stainless steel injectors or pulled glass micropipettes or (b) with fabricated SU-8 microinjectors, in a way that the fluid outlet is placed between the two sensor electrodes at a vertical distance of approximately 100 μm (described in Frey et al., 2010). Injections were performed using a precision 5-μl syringe controlled by a motorised pump (Hamilton Bonaduz AG, Switzerland) with a flow-rate of 500 nl/min when not otherwise stated. Two electrochemical set-ups were used: (a) a three-electrode configuration with a home-made, 125-μm thick Ag/AgCl reference electrode and a 100-μm thick Pt wire (99.99%, Aldrich) counter electrode or (b) the integrated Ag/AgCl electrode on the microprobe was used as combined reference/counter electrode in a two-electrode configuration.

All measurements were acute; i.e. biosensors remained in the brain for 4–8 h depending on the measurements performed. Once implanted the required potentials were applied. Experiments were started as soon as the signal reached a constant current level (settling curve, 30 min). Biosensors were calibrated immediately before and after their implantation. Concentration scale bars in graphs of Section 3 refer always to the calibration measurement performed before the tests.

Following the conclusion of each experiment rats were sacrificed with an overdose of sodium pentobarbitone (200 mg/ml) and perfused with 4% paraformaldehyde via the transcardiac route. Brains were removed, sectioned on a microtome and stained with Cresyl Violet.

3. Results and discussion

3.1. Microprobe arrays

Fig. 2-A shows a SEM micrograph of the front part of a single silicon microprobe with the two KOH-recessed electrodes and the larger reference electrode. The DRIE process allowed well-reproduced shape of the probe with respect to the designed masks (<2 μm accuracy). Very sharp tips facilitating the brain insertion were achieved.

An assessment of the quality of the Pt microelectrodes by cyclic voltammetry in 1 M H_2SO_4 solution showed good surface characteristics and a roughness factor of <2 determined using the hydrogen desorption charge (210 μC/cm^2, Bard and Faulkner, 2001). The AgCl layer on the larger electrode has a homogeneous thickness and good coverage of the underlaying Pt. A packaged 4-shaft comb is shown in Fig. 2-B.

3.2. Functionalisation—general remarks

Electrochemical aided adsorption highly qualifies for the functionalisation of microelectrodes in a three-dimensional configuration because it allowed to deposit well-localised membranes with incorporated choline oxidase, L-glutamate oxidase or simply BSA on dedicated electrodes in a very controlled way. Connecting several electrodes resulted in equal depositions on all electrodes. The exact mechanism of the electrodeposition is assumed to be either electrophoretically driven (Strike et al., 1995; Kim and Oh, 1996) or a consequence of local pH decrease (Matsumoto et al., 2002).

The deposition protocol, the concentration of the ingredients in the deposition solution and the microprobe pretreatment were optimised with respect to sensor performance, immobilisation efficiency and reproducibility. In comparison to previous published protocols, where several galvanostatic pulses were used (Strike et al., 1995; Frey et al., 2007a), a higher reproducibility was obtained using a series of potentiostatic pulses. It has the additional advantage, that the protocol has not to be adjusted when the all over coating surface is changing (e.g. for parallel depositions, larger electrodes). Duration and potential of the pulse are critical. The first, relatively high potential (5 s at 1.8 V) generates enough electrophoretic force to aggregate the negatively charged enzymes and protein for cross-linking with GA without electrochemical damage of the electrode metal. The no-effect, second potential (10 s at 0.4 V) reestablishes the bulk concentration near the electrode. The pulse time and quantity are a trade-off between very thin layers with low enzyme load (<2 s, <15 pulses) and uncontrollable membrane growth (>10 s). More than 25 pulses resulted in no further, significant sensor enhancement. The thickness of the membrane is approximately 8–10 μm.

As expected, the variation of the GA concentration at constant enzyme/protein concentrations has a strong influence on the sensitivity of the sensors as well as the pot life of the deposition solution. Low GA concentrations (<0.1%) produce very low or no immobilisation of the enzyme. Higher concentrations of GA (e.g. 2.5%) partially resulted in very high sensitivities of the biosensors (up to 27.7 pA/μM, corresponding to 370 μA mM^{-1} cm^{-2} for choline), but could not be practically used. Time between mixing of the solution and its complete cross-linking was less than 20 min and sometimes produced cluster-like structures overlapping the electrode not guaranteeing reproducibility and spatial control. For a GA concentration of 1% (v/v), the solution could be used for at least 2 h. Complete gelification occurred after about 6 h.

Silanisation with APTES is widely used for surface modification and immobilisation of biological elements (Subramanian et al., 1999). While it improves the adhesion of the enzymatic membrane to the electrode (Vandenberg et al., 1991), it enhances two important parameters: (a) storage and functional lifetime, and (b) reproducibility of enzyme deposition.

The *m*-PPD deposition protocol was optimised for the EAA-modified electrodes with respect to the AA-blocking properties of the electropolymerised layer. In contrast to other groups (Bruno et al., 2006; McMahon et al., 2006) using potentiostatic deposition, we observed best results and durability using cyclic voltammetry. It also has to be noted, that the layer is deposited after enzyme immobilisation and on active and inactive electrodes in parallel. A preceding deposition is not compatible with EAA (non-conduction layer) and further, Osborne and Hashimoto (2004) observed a good affinity of *m*-PPD with GA and immobilised enzymes.

3.3. In vitro characterisation

The obtained functional parameters for both, L-glutamate and choline biosensors are summarised in Table 1. Graphs A and B in Fig. 3 show typical calibration curves for respectively a choline and glutamate biosensor upon consecutive addition of neurotransmitter and interferant aliquots to reach concentrations in the expected range (Fillenz, 2005; Zhang and Mao, 2005). Measurements were performed on day one after the functionalisation of the microelectrode.

The sensitivities of 9.9 ± 1.5 pA/μM ($n = 16$) for the choline biosensor and 7.1 ± 1.5 pA/μM ($n = 20$) for the glutamate sensor are lower compared with results obtained with deposition solution formulations with higher GA concentrations and/or without silanisation (see supplementary data, Fig. SD2-B). However, reproducibility and lifetime could be substantially improved and sensitivities in the range of 10 pA/μM compare well with results obtained by other groups (Mitala and Michael, 2006; O'Neill et al., 2008; Burmeister et al., 2008). Further, the lower sensor performance resulting from the pretreatment with APTES is small compared to results from other groups reporting a 6–8-fold decrease of the sensitivity using a similar silanisation after enzyme immobilisation (Chen et al., 2002).

Table 1
Sensor *in vitro* characteristics.

Analytical property	Choline sensor Value ± S.D.	Glutamate sensor Value ± S.D.
Sensitivity	9.9 ± 1.5 pA/μM ($n = 16$)	7.1 ± 1.5 pA/μM ($n = 20$)
Linear response	300 μM ($R = 0.998$)	100 μM
Detection limit[a]	0.30 μM	0.42 μM
Response time		
$t_{90\%}$[b]	6 s	6 s
$t_{95\%}$	10 s	10 s
Temperature dependence[c]	2.2%/°C ($n = 16$)	1.9%/°C ($n = 9$)
Lifetime[d]	−0.1 pA μM^{-1} d^{-1}	∼Const. within exp. error
Oxygen dependence[e]	92 ± 11.2% ($n = 3$)	–

[a] 3 times the background noise.
[b] Measured in a specially developed microfluidic device allowing subsecond concentration changes (Frey et al., 2007b).
[c] Calculated by comparing calibration curves measured at 37 °C and room temperature.
[d] For the first two months (see Fig. SD2-A). Notwithstanding such long-term stability, calibration measurements have to be performed before *in vivo* use to determine the actual sensitivity.
[e] Measured in PBS solutions equilibrated with respectively 21%, 10% and 5% oxygen (Fig. SD2-D). The sensitivity decrease lies within previously published results (Burmeister et al., 2003; McMahon et al., 2006). This percentage represents the lower limit of the O_2 concentration expected in the extracellular brain fluid (Dixon et al., 2002).

Choline and glutamate biosensor calibration curves performed in artificial extracellular fluid (aECF) showed only slightly lower values with respect to the sensitivity (<10%), but similar behaviour with respect to the noise level and the lifetime.

3.4. Interference rejection

The deposition of the *m*-poly(phenylenediamine) layer resulted in a close to 100% rejection of dopamine (DA) and ascorbic acid (AA) (see for example Fig. 3-A and -B). The selectivity refers to a ratio of the neurotransmitters sensitivity over the interferants' such as AA ($Sens_{NT}/Sens_{AA}$). Selectivity ratios over 100:1 (=99% rejection) are desirable, but ratios of 20:1 (=95%) are still acceptable and were determined as the minimal rejection ratio for *in vivo* measurements. For an electrode with a selectivity below 100% (Fig. 3-A), complete elimination of the interfering signals can be achieved using the differential method (solid curve).

A slight decrease (−3%) of the rejection properties of the *m*-PPD layer was observed during the first two weeks of the biosensor lifetime (cf. Burmeister et al., 2008). The results of two batches of choline biosensors ($n = 4$–6 for each batch) and two batches of glutamate biosensors are shown in Fig. SD2-C. However, all biosensors show average rejection rates over 30:1 (=96.6%). *m*-PPD degradation may be caused by a locally high H_2O_2 concentration. Long-term stability for chronic use has to be further investigated.

It has to be noted, that beside the possibility to completely eliminate interferences, the differential method allows also to substantially reduce external influences such as electrical noise or artefacts.

3.5. Parallel depositions and reproducibility

Fig. 3-C shows off-setted, parallel-recorded *in vitro* response curves of four simultaneously coated electrodes by biasing the four front electrodes on a 4-shaft comb. The result shows identical characteristics for all single biosensor regarding sensitivity and anti-interference characteristics, emphasising the reproducibility of the deposition method and its compatibility for large-scale integration.

When electrodes were coated in parallel a variation of the sensitivities for choline was 6.8% on average ($n = 8$) and 8.6% for glutamate biosensors ($n = 6$). In the example in Fig. 3-C the average choline sensitivity is 6.1 ± 0.1 pA/μM ($n = 4$), i.e. a variation of less than 2%.

3.6. Spatial control and cross-talk

As mentioned above, the EAA method is perfectly suited to coat closely spaced electrode sites. Fig. 3-D shows the response of a microprobe, where one electrode of the microprobe is coated with choline oxidase and the second with glutamate oxidase. Each electrode responds to only the corresponding injection of respectively choline or glutamate samples. This measurement illustrates, that the immobilisation method is first, not sensitive to cross-contamination or unspecific adsorption during serial enzyme depositions and second, no cross-talk is observed during the measurement for two electrodes separated by 200 μm. The absence of cross-talk is also confirmed in Fig. 3-A and -B.

3.7. In vivo characterisation

The following *in vivo* measurements aim to demonstrate the proper function of the developed microprobe biosensors prepared by the above-described procedure and chosen for *in vivo* use upon criteria similar to other groups (Bruno et al., 2006; Michael and Borland, 2007).

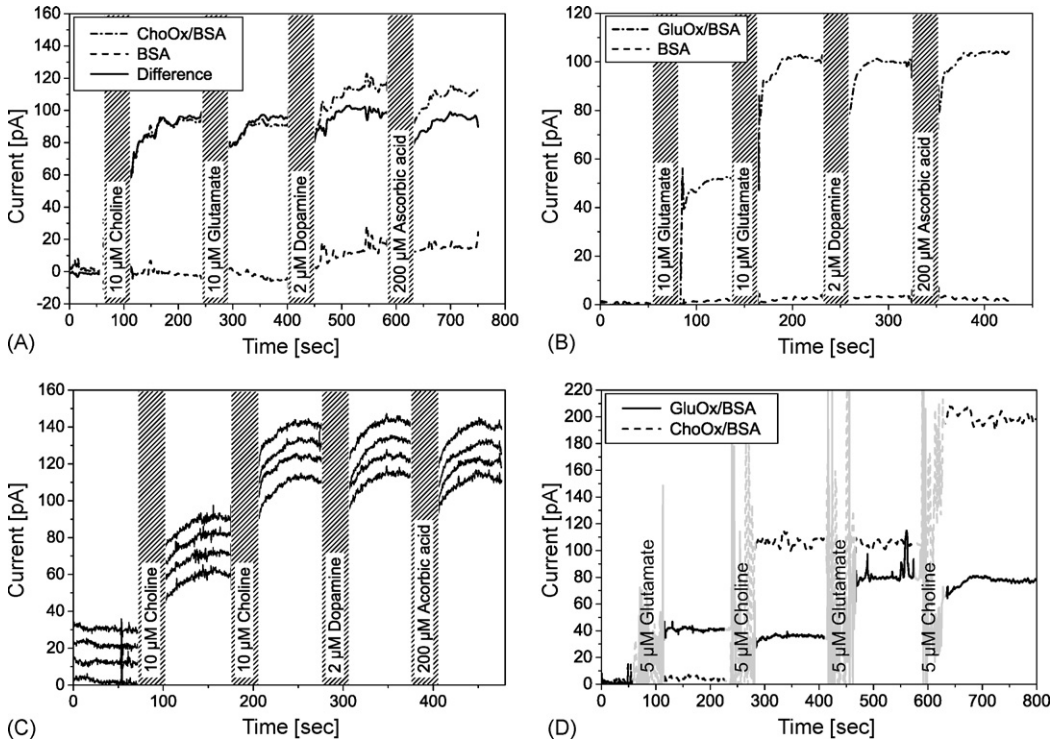

Fig. 3. (A) Response of a choline biosensor upon consecutive additions of choline (10 μM), glutamate (10 μM), dopamine (2 μM) and ascorbic acid (200 μM). The dash-dotted trace represents raw-data of the enzyme electrode, the dashed trace of the control electrode (recorded at 37 °C). The solid trace shows the difference and the complete removal of interferant contributions. (B) Response of a glutamate biosensor upon consecutive additions of glutamate (2 × 10 μM), dopamine (2 μM) and ascorbic acid (200 μM). The curve was recorded in PBS at room temperature. (C) Raw-data of a parallel *in vitro* recording of four simultaneously coated choline biosensors on a 4-shaft comb (curves are separated by 10 pA for better visibility). (D) Response of choline (dashed) and glutamate biosensor (solid) on a single microprobe separated by 200 μm upon additions of 5 μM glutamate and choline, respectively. Sensitivities are 20.0 pA/μM for the choline and 8.1 pA/μm for the glutamate biosensor (non-optimised deposition solution used here).

Initial experiments consisted of the local delivery of the specific neurotransmitter in the vicinity of the biosensor. The aim was to verify, if the biosensor is able to detect the externally injected molecule in the neural environment and can discriminate between different concentration increases. Fig. 4 shows the raw-data of a choline biosensor (A) and a glutamate biosensor (B). In both cases the single microprobe was assembled with a 31-gauge stainless steel injector. The outlet was positioned between the two modified microelectrodes with a vertical distance of around 100 μm for the choline and 50 μm for the glutamate sensor.

Both graphs show graded responses of the choline and glutamate biosensors to injections of a 200 mM choline and glutamate solutions, respectively. The apparent non-linearity of the responses can have several causes: (a) it may reflect signal saturation at the relatively high doses of choline/glutamate employed and the non-linear concentration distribution of the diffusion controlled neurotransmitter dispersion, (b) arise from transmitter induced transmitter release, causing an avalanche of local neural activity which might last a long time and produce its own increases in choline and glutamate concentration. Nevertheless, the signals were very stable and highly reproducible. Signal amplitudes are strongly depending on the biosensor/injector separation and the local diffusion and neurotransmitter clearance in the brain. Therefore it is very difficult to compare different experiments which each other.

Endogenous choline concentrations were detected in two different experiments: KCl-induced ACh release was repeatedly measured in the mPFC by detection of choline—the break-down product of ACh generated by a reaction involving acetylcholinesterase (AChE). A choline biosensor microprobe combined with a glass capillary used as injector was implanted at the following stereotaxic coordinates: A/P 1.7 mm, M/L 0.7 mm, D/V 3 mm.

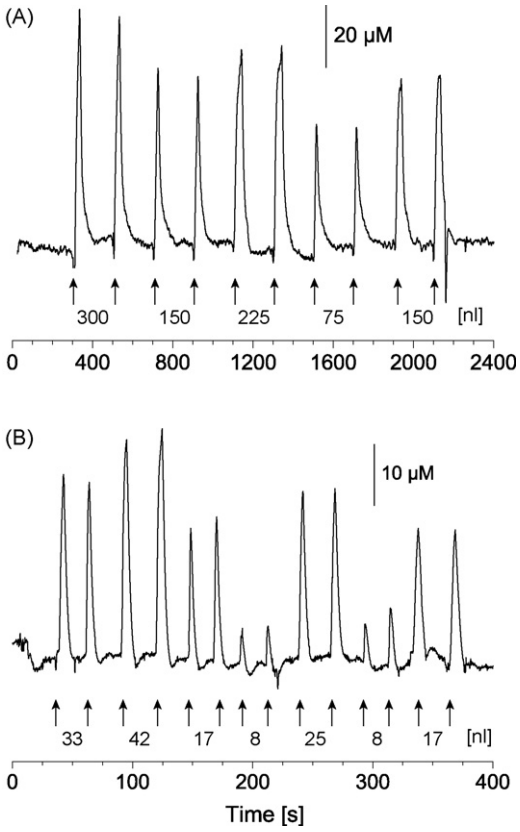

Fig. 4. Raw-data of the recorded signals of a choline (A) and a glutamate sensor (B) in the PFC upon volume-varied injections of the specific neurotransmitter solution.

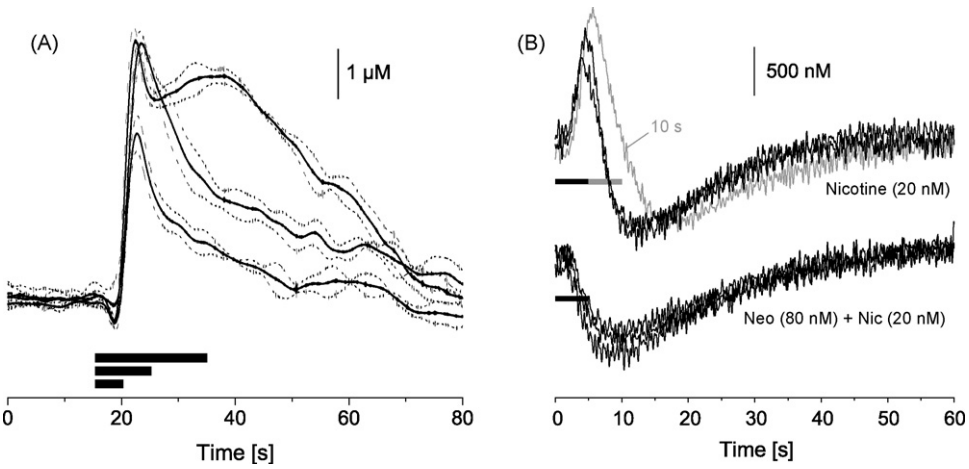

Fig. 5. KCl and nicotine evoked ACh release: (A) response curve upon injections of different volumes of KCl (70 mM). (B) Nicotine-induced ACh release and subsequent inhibition of ACh hydrolysis via AChE using neostigmine. Curves were recorded using the differential method having the signal of the inactive control electrode already subtracted.

Three different volumes of 70 mM KCl solution were injected at a flow-rate of 750 nl/min (injection time is marked by a horizontal bar; volumes are 63, 125 and 250 nl). Fig. 5-A presents the recorded response of the biosensor. Each curve represents the average (solid trace) and standard deviation (dashed traces) over three repeated injections at each volume. As expected, the three different volumes resulted in a variation of ACh release. The time and concentration range of the response are comparable with other published data (Mitchell, 2004). Similarly, signal shape and amplitude strongly depends on the chosen injection parameters.

In a different experiment, we reproduced a double-injection protocol that has already been carried out by other groups (Parikh et al., 2004; Bruno et al., 2006). Nicotine (20 nM in filtered 10 mM PBS) was used to evoke a presynaptic ACh release in the PFC (coordinates: A/D 2.5 mm, M/L 1 mm, D/V 3 mm). A volume of ~1 μl was infused over a time of 5 and 10 s and the variation in choline concentration was measured by an adjacently placed choline biosensor (upper traces in Fig. 5-B). The interval time was 90 s. The first injection of ~1 μl was performed over 10 s, all other over 5 s. The chemical stimulation resulted in a detectable release of ACh. Subsequently, neostigmine (80 nM in filtered 10 mM PBS) – a known inhibitor of AChE – was infused (2 μl over 30 s) into the same brain area using the second channel of a SU-8 microinjector. 20 min later, another three nicotine injections were performed (lower traces). This time, no current increase could be detected in the choline biosensor signal. Neostigmine efficiently inhibited AChE demonstrating that choline signals are dependent upon the hydrolysis of ACh via AChE and giving evidence, that previously detected choline signals are a direct result of the nicotine stimulation.

In the experiment, rather small concentrations of nicotine and neostigmine were used. This required the injection of comparably large volumes over a short time period to evoke a detectable concentration change. The decrease of all 6 current signals may result from a temporary dilution of the local ECF or the high flow-rate might have caused a volume displacement of the local brain tissue.

4. Conclusions

We presented the fabrication of silicon microprobe arrays fulfilling the requirements for brain implantation including microprobe dimensions, mechanical stability, Pt-microelectrode quality and application-specific design. The developed functionalisation method for the deposition of the enzymatic membranes and anti-interference layers on the microelectrodes allows (a) a parallel deposition and is compatible with two- and three-dimensional microprobe arrays comprising several microelectrodes for local monitoring in different brain regions and (b) creation of closely spaced multi-biosensor arrays for simultaneous measurement of different analytes in the same area without cross-talk. This feasibility was demonstrated on single microprobes and combs providing evidence of adequate biosensor performances for the detection of choline and L-glutamate in the physiologically relevant concentration ranges. The next step will be to translate our biosensor technology into a package suitable for use in awake, behaving animals.

Acknowledgements

This work is supported by the European integrated project NeuroProbes (EU IP IST-027017). The authors gratefully thank the staff at the Microsystems Technology Division of the CSEM, Neuchâtel, Switzerland, for support during the fabrication process.

Appendix A. Supplementary data

Supplementary data associated with this article can be found, in the online version, at doi:10.1016/j.bios.2010.07.073.

References

Aarts, A.A.A., Neves, H.P., Puers, R.P., Van Hoof, C., 2008. J. Micromech. Microeng. 18, 064004 (7 pp.).
Bard, A.J., Faulkner, L.R., 2001. Electrochemical Methods: Fundamentals and Applications, 2nd ed. Wiley, New York.
Bruno, J.P., Gash, C., Martin, B., Zmarowski, A., Pomerleau, F., Burmeister, J., Huettl, P., Gerhardt, G.A., 2006. Eur. J. Neurosci. 24 (10), 2749–2757.
Burmeister, J.J., Moxon, K., Gerhardt, G.A., 2000. Anal. Chem. 72 (1), 187–192.
Burmeister, J.J., Pomerleau, F., Palmer, M., Day, B.K., Huettl, P., Gerhardt, G.A., 2002. J. Neurosci. Methods 119 (2), 163–171.
Burmeister, J.J., Palmer, M., Gerhardt, G.A., 2003. Anal. Chim. Acta 481 (1), 65–74.
Burmeister, J.J., Pomerleau, F., Huettl, P., Gash, C.R., Werner, C.E., Bruno, J.P., Gerhardt, G.A., 2008. Biosens. Bioelectron. 23 (9), 1382–1389.
Chen, X., Matsumoto, N., Hu, Y., Wilson, G.S., 2002. Anal. Chem. 74 (2), 368–372.
Cheung, K.C., Djupsund, K., Dan, Y., Lee, L.P., 2003. J. Microelectromech. Syst. 12 (2), 179–184.
Cosnier, S., 2003. Anal. Bioanal. Chem. 377 (3), 507–520.
Cosnier, S., Innocent, C., Allien, L., Poitry, S., Tsacopoulos, M., 1997. Anal. Chem. 69 (5), 968–971.
Dixon, B.M., Lowry, J.P., O'Neill, R.D., 2002. J. Neurosci. Methods 119 (2), 135–142.
Ensell, G., Banks, D.J., Richards, P.R., Balachandran, W., Ewins, D.J., 2000. Med. Biol. Eng. Comput. 38 (2), 175–179.
Errachid, A., Ivorra, A., Aguilo, J., Villa, R., Zine, N., Bausells, J., 2001. Sens. Actuators B 78 (1–3), 279–284.
Fillenz, M., 2005. Neurosci. Biobehav. Rev. 29 (6), 949–962.
Frey, O., van der Wal, P., de Rooij, N.F., Koudelka-Hep, M., 2007a. Conf Proc IEEE Eng Med Biol Soc, Lyon, France, pp. 6040–6043.

Frey, O., Falke, F., van der Wal, P., de Rooij, N.F., Koudelka-Hep, M., 2007b. 11th Int. Conf. on Miniaturized Systems for Chemistry and Life Science (microTAS), vol. 2, Paris, pp. 1288–1290.
Frey, O., Holtzman, T., McNamara, R.M., Theobald, D.E., van der Wal, P.D., de Rooij, N.F., Dalley, J.W., Koudelka-Hep, M., 2010. Sens. Actuators B, doi:10.1016/j.snb.2010.01.034.
Garguilo, M.G., Huynh, N., Proctor, A., Michael, A.C., 1993. Anal. Chem. 65 (5), 523–528.
Geise, R.J., Adams, J.M., Barone, N.J., Yacynych, A.M., 1991. Biosens. Bioelectron. 6 (2), 151–160.
Gray, C.M., Maldonado, P.E., Wilson, M., McNaughton, B., 1995. J. Neurosci. Methods 63 (1–2), 43–54.
Guerrieri, A., Palmisano, F., 2001. Anal. Chem. 73 (13), 2875–2882.
Hanefeld, U., Gardossi, L., Magner, E., 2009. Chem. Soc. Rev. 38 (2), 453–468.
Herwik, S., Kisban, S., Aarts, A.A.A., Seidl, K., Girardeau, G., Benchenane, K., Zugaro, M.B., Wiener, S.I., Paul, O., Neves, H.P., Ruther, P., 2009. J. Micromech. Microeng. 19, 074008 (11 pp.).
Hu, Y.B., Mitchell, K.M., Albahadily, F.N., Michaelis, E.K., Wilson, G.S., 1994. Brain Res. 659 (1–2), 117–125.
Johnson, K.W., 1991. Sens. Actuators B 5 (1–4), 85–89.
Kewley, D.T., Hills, M.D., Borkholder, D.A., Opris, I.E., Maluf, N.I., Storment, C.W., Bower, J.M., Kovacs, G.T.A., 1997. Sens. Actuators A 58 (1), 27–35.
Khan, A.S., Michael, A.C., 2003. Trends Anal. Chem. 22 (9), 503–508.
Kim, C.S., Oh, S.M., 1996. Electrochim. Acta 41 (15), 2433–2439.
Kulagina, N.V., Shankar, L., Michael, A.C., 1999. Anal. Chem. 71 (22), 5093–5100.
Kurzawa, C., Hengstenberg, A., Schuhmann, W., 2002. Anal. Chem. 74 (2), 355–361.
Lada, M.W., Vickroy, T.W., Kennedy, R.T., 1997. Anal. Chem. 69 (22), 4560–4565.
Lee, J.S., Nakahama, S., Hirao, A., 1991. Sens. Actuators B 3 (3), 215–219.
Leong, K.H., Ensell, G., Wall, P., Pickard, R.S., 1990. Biosens. Bioelectron. 5 (4), 303–310.
Lowry, J.P., Miele, M., O'Neill, R.D., Boutelle, M.G., Fillenz, M., 1998. J. Neurosci. Methods 79 (1), 65–74.
Madou, M., 1997. Fundamentals of Microfabrication. CRC Press, Boca Raton, FL.
Malitesta, C., Palmisano, F., Torsi, L., Zambonin, P.G., 1990. Anal. Chem. 62 (24), 2735–2740.
Matsumoto, N., Chen, X., Wilson, G.S., 2002. Anal. Chem. 74 (2), 362–367.
McMahon, C.P., Rocchitta, G., Serra, P.A., Kirwan, S.M., Lowry, J.P., O'Neill, R.D., 2006. Anal. Chem. 78 (7), 2352–2359.
Michael, A.C., Borland, L.M., 2007. Electrochemical Methods for Neuroscience. CRC Press, Boca Raton, FL.
Mikeladze, E., Schulte, A., Mosbach, M., Blochl, A., Csoregi, E., Solomonia, R., Schumann, W., 2002. Electroanalysis 14 (6), 393–399.
Mitala, J.J., Michael, A.C., 2006. Anal. Chim. Acta 556 (2), 326–332.
Mitchell, K.M., 2004. Anal. Chem. 76 (4), 1098–1106.
Musallam, S., Bak, M.J., Troyk, P.R., Andersen, R.A., 2007. J. Neurosci. Methods 160 (1), 122–127.
Najafi, K., Wise, K.D., Mochizuki, T., 1985. IEEE Trans. Electron Devices 32 (7), 1206–1211.
Newman, J.D., Turner, A.P.F., Marrazza, G., 1992. Anal. Chim. Acta 262 (1), 13–17.
Niwa, O., Horiuchi, T., Kurita, R., Torimitsu, K., 1998. Anal. Chem. 70 (6), 1126–1132.
Norlin, P., Kindlundh, M., Mouroux, A., Yoshida, K., Hofmann, U.G., 2002. J. Micromech. Microeng. 12 (4), 414–419.
O'Neill, R.D., Lowry, J.P., Rocchitta, G., McMahon, C.P., Serra, P.A., 2008. Trends Anal. Chem. 27 (1), 78–88.
Osborne, P.G., Hashimoto, M., 2004. Analyst 129 (8), 759–765.
Parikh, V., Pomerleau, F., Huettl, P., Gerhardt, G.A., Sarter, M., Bruno, J.P., 2004. Eur. J. Neurosci. 20 (6), 1545–1554.
Qin, S., van der Zeyden, M., Oldenziel, W.H., Cremers, T.I.F.H., Westerink, B.H.C., 2008. Sensors 8 (11), 6860–6884.
Robinson, D.L., Hermans, A., Seipel, A.T., Wightman, R.M., 2008. Chem. Rev. 108, 2554–2584.
Ryan, M.R., Lowry, J.P., O'Neill, R.D., 1997. Analyst 122 (11), 1419–1424.
Sarma, A.K., Vatsyayan, P., Goswami, P., Minteer, S.D., 2009. Biosens. Bioelectron. 24 (8), 2313–2322.
Schuvailo, O.N., Dzyadevych, S.V., El'skaya, A., Gautier-Sauvigne, S., Csoregi, E., Cespuglio, R., Soldatkin, A.P., 2005. Biosens. Bioelectron. 21 (1), 87–94.
Strike, D.J., De Rooij, N.F., Koudelka-Hep, M., 1995. Biosens. Bioelectron. 10 (1–2), 61–66.
Subramanian, A., Kennel, S.J., Oden, P.I., Jacobson, K.B., Woodward, J., Doktycz, M.J., 1999. Enzyme Microb. Technol. 24, 26–34.
Takahashi, K., Matsuo, T., 1984. Sens. Actuators 5 (1), 89–99.
Ulbert, I., Halgren, E., Heit, G., Karmos, G., 2001. J. Neurosci. Methods 106 (1), 69–79.
Vandenberg, E., Elwing, H., Askendal, A., Lundstrom, I., 1991. J. Colloid Interface Sci. 143 (2), 327–335.
Wassum, K.M., Tolosa, V.M., Wang, J.J., Walker, E., Monbouquette, H.G., Maidment, N.T., 2008. Sensors 8 (8), 5023–5036.
Wilson, G.S., Gifford, R., 2005. Biosens. Bioelectron. 20, 2388–2403.
Wise, K.D., Angell, J.B., Starr, A., 1970. IEEE Trans. Biomed. Eng. BM17 (3), 238–247.
Xin, Q., Wightman, R.M., 1997. Anal. Chim. Acta 341 (1), 43–51.
Yoon, T.H., Hwang, E.J., Shin, D.Y., Park, S.I., Oh, S.J., Jung, S.C., Shin, H.C., Kim, S.J., 2000. IEEE Trans. Biomed. Eng. 47 (8), 1082–1087.
Yoshida, S., Kanno, H., Watanabe, T., 1995. Anal. Sci. 11 (2), 251–256.
Zhang, M.N., Mao, L.Q., 2005. Front. Biosci. 10, 345–352.